This is an open access article published under an ACS AuthorChoice License, which permits copying and redistribution of the article or any adaptations for non-commercial purposes.

Environmental Science & Technology

Article

pubs.acs.org/est

Improved Mechanistic Understanding of Natural Gas Methane Emissions from Spatially Resolved Aircraft Measurements

Stefan Schwietzke,*[,†,‡] Gabrielle Pétron,[†,‡] Stephen Conley,[§,∥] Cody Pickering,[⊥] Ingrid Mielke-Maday,[†,‡] Edward J. Dlugokencky,[‡] Pieter P. Tans,[‡] Tim Vaughn,[⊥] Clay Bell,[⊥] Daniel Zimmerle,[⊥] Sonja Wolter,[†,‡] Clark W. King,[‡] Allen B. White,[‡] Timothy Coleman,[†,‡] Laura Bianco,[†,‡] and Russell C. Schnell[‡]

[†]Cooperative Institute for Research in Environmental Sciences, University of Colorado, 216 UCB, Boulder, Colorado 80309, United States

[‡]NOAA Earth System Research Laboratory, 325 Broadway, Boulder, Colorado 80305, United States

[§]Scientific Aviation, Inc., 3335 Airport Road Suite B, Boulder, Colorado 80301, United States

[∥]Department of Land, Air, and Water Resources, University of California, One Shields Avenue, Davis, California 95616, United States

[⊥]Department of Mechanical Engineering, Colorado State University, 400 Isotope Dr, Fort Collins, Colorado 80521, United States

Supporting Information

ABSTRACT: Divergence in recent oil and gas related methane emission estimates between aircraft studies (basin total for a midday window) and emissions inventories (annualized regional and national statistics) indicate the need for better understanding the experimental design, including temporal and spatial alignment and interpretation of results. Our aircraft-based methane emission estimates in a major U.S. shale gas basin resolved from west to east show (i) similar spatial distributions for 2 days, (ii) strong spatial correlations with reported NG production (R^2 = 0.75) and active gas well pad count (R^2 = 0.81), and (iii) 2× higher emissions in the western half (normalized by gas production) despite relatively homogeneous dry gas and well characteristics. Operator reported hourly activity data show that midday episodic emissions from manual liquid unloadings (a routine operation in this basin and elsewhere) could explain ∼1/3 of the total emissions detected midday by the aircraft and ∼2/3 of the west−east difference in emissions. The 22% emission difference between both days further emphasizes that episodic sources can substantially impact midday methane emissions and that aircraft may detect daily peak emissions rather than daily averages that are generally employed in emissions inventories. While the aircraft approach is valid, quantitative, and independent, our study sheds new light on the interpretation of previous basin scale aircraft studies, and provides an improved mechanistic understanding of oil and gas related methane emissions.

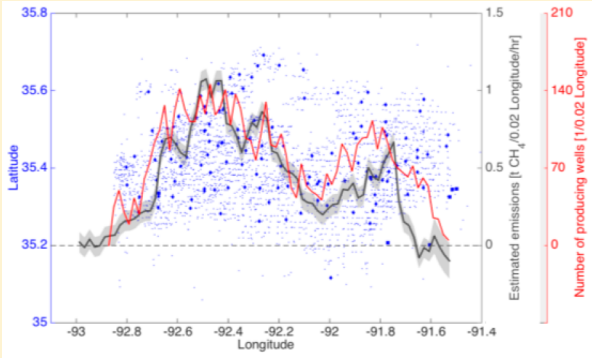

INTRODUCTION

Reducing the amount of leaked and vented natural gas (NG) during its production, processing, transport, and use has become a high priority in U.S. efforts to cut anthropogenic emissions of methane (CH_4) and in some cases also of nonmethane hydrocarbons that can cause tropospheric ozone pollution or pose direct health risks.[1] Tracking and evaluating the performance of different operational and mitigation measures requires (i) a better understanding of these emissions including accurate baselines and (ii) robust quantification methods.

Different measurement-based approaches have recently been applied toward this end, including basin-level total emission quantification using aircraft, i.e., top-down,[2−9] as well as facility- and component-level emission quantification and characterization for a subset of operations using a variety of engineering calculations or ground-based measurement techniques, i.e., bottom-up.[10−14] The latter have been used to generate and update CH_4 emission inventories for national emission reporting.[15] The resulting body of literature shows systematic discrepancies where top-down estimates are substantially greater than bottom-up estimates.[16] Interpretation of this discrepancy is difficult because few studies provide data that are complete (measurement sample count relative to population), independent (based only on measurements rather than industry reported data based on engineering estimates), and temporally and spatially consistent (e.g., covering the same exact sites at

Received: April 7, 2017
Revised: May 26, 2017
Accepted: May 26, 2017
Published: May 26, 2017

Downloaded via 207.241.233.247 on October 24, 2020 at 23:30:21 (UTC).
See https://pubs.acs.org/sharingguidelines for options on how to legitimately share published articles.

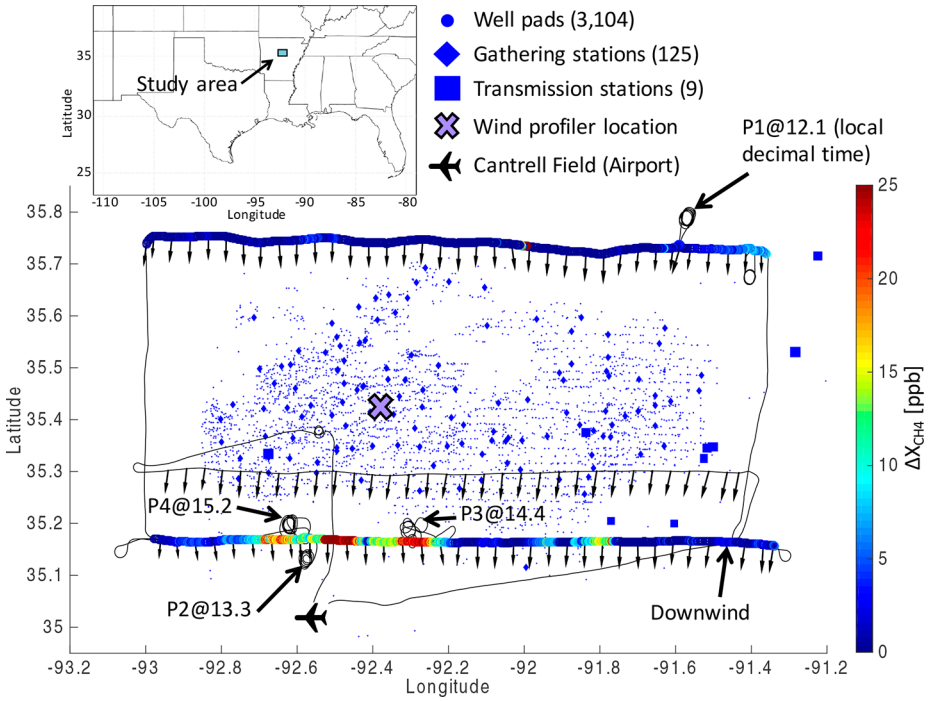

Figure 1. Overview of October 1, 2015 flight track (approximately 150 km west−east and 65 km north−south, black and line color-coded by CH_4 mole fractions relative to background (ΔX_{CH_4}) along upwind and downwind transects). The arrows show 1 min average aircraft measured wind speed (mean 7.8 m/s) and direction (mean 2° N). The October 2 flight includes a partial transect further south (35.1° latitude) in addition to a full transect at 35.15° latitude to demonstrate that potential downwind CH_4 plumes from nearby well pads (−92.1° to −91.8° longitude) were negligible (Figure S2b and Figure S3). Local time indicates Central Daylight Time (UTC−5). Figure was produced using MATLAB.[43]

the same time, and incorporating other temporal emission variability such as episodic maintenance events) to allow a consistent emission comparison of estimates from both approaches. For example, the EPA's Greenhouse Gas Inventory[15] is based on annual emission averages, whereas aircraft emission estimates are for the period during which measurements are taken (mostly midday when the planetary boundary layer (PBL) is fully grown and well-mixed).

Our paper is part of a comprehensive study to expand and improve the top-down vs bottom-up reconciliation effort by providing for the first time a spatially resolved aircraft-based midday CH_4 emission estimate for comparison with a temporally and spatially consistent bottom-up inventory.[17] The latter is based on a larger sample size and more comprehensive set of facility-level measurement methods (downwind on the ground and with aircraft, and on-site) than previous work.[18]

In this paper, we quantify spatially resolved CH_4 emissions using the aircraft mass balance method, which has been applied previously to quantify total area emissions of CH_4 (refs 3−6, 9), C_2H_6 (refs 2, 7), and black carbon[8] (a product of incomplete combustion including NG flaring) from U.S. oil and gas basins for comparison with emission inventories. This approach has also been applied to quantify urban fossil fuel CO_2 emissions.[19] As described in detail below, this method integrates measured trace gas mole fraction "enhancements" (ΔX_{CH_4}) in the PBL downwind of sources relative to the CH_4 measured upwind. We further refined the mass balance method by explicitly accounting for nonuniform upwind CH_4 mole fractions in the PBL entering the study area in order to estimate unbiased CH_4 emissions from individual study area subsections (see below and Materials and Methods section). Other methods exist that rely on more complex plume dispersion models,[20] which have been applied to quantify emissions from other trace gases and sources. The application of such methods is useful during more heterogeneous atmospheric conditions than in our study or when quantifying emissions from point sources.

The Fayetteville Shale in northern central Arkansas (Figure 1) was one of the first economically significant shale gas plays to be developed in the U.S. (second largest shale gas production[21] after the Barnett Shale, TX until 2009). It is a dry gas play, i.e., producing no oil. Studying a dry gas play bypasses the challenge[22] of having to attribute CH_4 emissions between oil and NG when calculating a production normalized emission rate (PNER, defined as the percentage of produced CH_4 released to the atmosphere including emissions due to leaks and by design). Prior to this study, Peischl et al.[6] had quantified CH_4 emissions top-down from the same Fayetteville region during one flight in June 2013 when the average NG production of 2.7 billion cubic feet per day (bcfd)[6] was slightly higher than during our study period (2.5 bcfd).[23] In the same geographic domain, we performed 15 flights (all on separate days) between September 21 and October 14, 2015, including two flights (October 1 and 2) for estimating total study area CH_4 emissions. The remaining 13 flights did not meet the meteorological prerequisites for the aircraft mass balance method. However, the meteorological conditions on these 13 flights were sufficient to sample study-area-wide ethane (C_2H_6) to CH_4 ratios for CH_4 emission source attribution as well as to quantify facility-level CH_4 emissions, which is described in companion papers.[24,25]

DOI: 10.1021/acs.est.7b01810
Environ. Sci. Technol. 2017, 51, 7286−7294

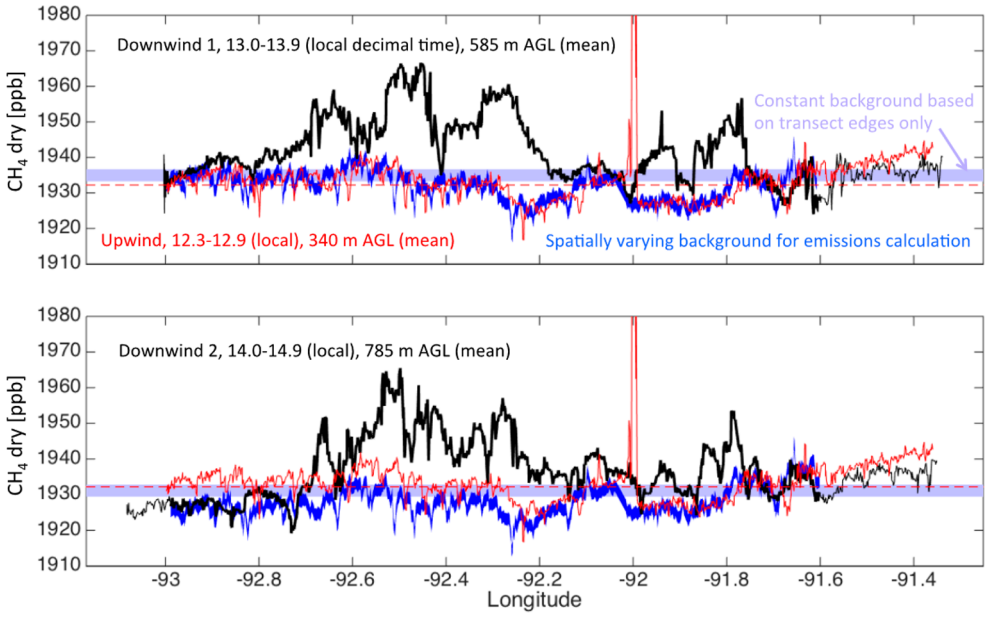

Figure 2. Study area upwind (red) and two downwind (black) transect CH_4 mole fractions measured on October 1, 2015 excluding the vertical profiles, which are shown in Figure S11. The spatially varying CH_4 background (blue), which equals the nonuniform upwind CH_4 shifted longitudinally according to mean wind direction across the study area (see text and Figure S4a), was used in the CH_4 emission calculation. The violet bar shows the CH_4 background (including uncertainties) as defined using the method in most previous aircraft mass balance studies.[2−5,7] See text for discussion of the upwind CH_4 spike near 92.0° longitude (12.5 CDT; maximum 2009 ppb CH_4 beyond *y*-axis maximum), which was manually removed from the spatially varying CH_4 background. Local time indicates Central Daylight Time (UTC−5). Figure was produced using MATLAB.[43]

■ MATERIALS AND METHODS

Measurement Platforms and Measured Parameters. The flights were performed with a single engine Mooney Ovation aircraft,[26] which collects onboard GPS and horizontal wind speed/direction data as described in Conley et al.[27] We measured *in situ* CH_4, carbon dioxide (CO_2), and water vapor (H_2O) using a Picarro model 2301-f wavelength-scanned cavity ring-down spectrometer (WS-CRDS) sampling every 2 s. *In situ* H_2O data were used to calculate[28] CH_4 and CO_2 mole fractions in dry air because those are the quantities that are conserved during transport (see details in SI section 1), and CH_4 and CO_2 calibrations were performed at NOAA in Boulder, CO, using compressed gas cylinders at six different mole fractions spanning ambient air on the WMO CH_4 X2004A standard calibration scale.[29,30] Target tank measurements performed on the ground after each flight indicated small day-to-day drift (1.1 ppb, 1σ) in the measured mole fractions. We also measured *in situ* C_2H_6 on the aircraft (see ref 31 for instrumentation), and the data are described in Mielke-Maday et al.[24] including additional analyses of the source attribution for the CH_4 emissions estimated here.

A 915-MHz Boundary-layer Radar Wind Profiler (BLWP) was deployed and operated near Bee Branch, AR (35.43° N, 92.38° W; within the study area) for the duration of the campaign. The BLWP is a pulsed-Doppler radar,[32] and the literature[33] provides a detailed description for producing 5 min averaged wind speed and direction hourly as well as diagnostics of the height of the convective boundary layer (all at 60- or 100-m vertical resolution from near the surface, 180 m, to as high as 4−5 km above ground level).

Refined Study Area Aircraft Mass Balance Approach. The mass balance[34] study-area-wide CH_4 emissions, E_{CH_4}, were calculated as

$$E_{CH_4} = \int_{-b}^{b} \Delta X_{CH_4} v \cos\theta \, dx \int_{z_{Ground}}^{z_{PBL}} n_{air,dry} \, dz \quad (1)$$

where ΔX_{CH_4} and v are the CH_4 mole fraction measurements relative to background and horizontal wind speed, respectively, integrated over each plume width increment ($-b$ to b; here along west to east upwind and downwind transect) corrected for the mean wind direction normal to the flight track ($\cos\theta$ dx), and $n_{Air,dry}$ accounts for measured dry air molar density (to compute CH_4 emissions in mass units based on measured CH_4 mole fractions) across the vertical from ground elevation (z_{Ground}) to the PBL top (z_{PBL}).

We further refined the aircraft mass balance approach including (i) an in-depth exploration of the sensitivity of downwind ΔX_{CH_4} and total CH_4 emissions to the definition of background CH_4 entering the study area, (ii) taking into account the vertical and horizontal wind gradients, and (iii) characterizing the longitudinal CH_4 emission distribution throughout the study area. We estimate the background CH_4 mole fractions for each downwind transect based on the CH_4 mole fractions at both edges of the downwind transect plume and along the transect upwind of the study region (see Figure 2 and Results). We calculated average horizontal wind speed and direction (and their uncertainties) for each plume width increment b based on aircraft measurements along each transect throughout the study area as well as wind profiler data (see Figure S12 for details), the latter accounting for variability in the vertical. Accounting for the resulting west to east (W-E) wind speed gradient (Figure S13) in the CH_4 emission calculation is important because the estimated CH_4 emissions of each section along the downwind transect depend not only on the local ΔX_{CH_4} but also on the local horizontal wind speeds throughout the PBL (see Methods eq 1). Also, using average wind speeds in the CH_4 emission calculation

DOI: 10.1021/acs.est.7b01810
Environ. Sci. Technol. 2017, 51, 7286−7294

despite an observed W-E wind speed gradient would bias total CH_4 emission because the observed ΔX_{CH_4} was not uniform from west to east. The methods for estimating uncertainties of all parameters and propagating them are described in SI section 6.

Multiple aircraft downwind transects were sampled temporally between 13.0 and 17.0 (all times indicate local decimal time; Central Daylight Time (CDT) or UTC−5) to allow for complete vertical mixing of near surface emissions throughout the planetary boundary layer (PBL) when sampled along study area downwind transects. We also demonstrate—using wind profiler time series (Figure S12)—that atmospheric transport prior to each flight was sufficient to "flush" the study area of any potential surface accumulations of CH_4 emissions (often at night) that would otherwise bias estimated CH_4 emissions. Aircraft vertical profiles were performed on most flights, except on October 2, but meteorological conditions were very similar to October 1 (Figure S12), to demonstrate a well-mixed PBL such that sampled air is vertically representative of the PBL during each transect, and to determine PBL height (in addition to wind profiler data collected on all days).

Flight Overview of October 1, 2015. A summary of the October 1 flight track is shown in Figure 1, which defines our study area (see the equivalent Figure S2 for October 2, and Figure S4 for flight tracks of all flights including those for source allocation facility-level CH_4 emissions quantification). Starting from Cantrell Field airport near Conway, AR, the aircraft started sampling the upwind transect at the northeastern corner of the flight track given the northerly winds, and heading west in the PBL.

The first aircraft vertical profile (P1 in Figure 1) was performed at the beginning of the upwind transect around noon, which indicated a well-mixed PBL, i.e., no vertical gradient in the observed CH_4 dry air mole fraction (Figure S8). The first W-E downwind transect along approximately 35.18° latitude and a nearly constant altitude of ∼600 m above ground level (AGL) followed directly after the upwind transect between 13−14 CDT. Vertical profile (P2) measurements were performed in peak ΔX_{CH_4} of the downwind plume (PBL height 1230 ± 100 m; see Figure S8). This downwind transect was repeated twice at the same latitude, but at altitudes between 800 and 1000 m AGL, also including one vertical profile each. A last transect inside the study area (35.30° latitude at mean 617 m AGL, 16−17 CDT) provided additional wind measurements along with the wind profiler data (see Methods) indicating largely consistent horizontal winds throughout the study area from north to south (Figures S12 and S13).

Clear skies throughout the study area and flight time window (11−17 CDT) as well as surface temperatures of 27 °C promoted development of convective eddies, assuring a well-mixed PBL (Figure S8). The PBL had its largest growth (i.e., deepening of the PBL) until noon CDT followed by another 15% PBL growth until the end of the flight (17 CDT) on October 1 (Figure S2a), which is accounted for in the CH_4 emission estimation (see below).

■ RESULTS

Detailed Analysis of October 1, 2015 Measurements. The October 1, 2015 CH_4 mole fractions in the upwind transect and the downwind transects 1 and 2, which were used to calculate total study area emissions, are shown in Figure 2 (see SI section 2 for equivalent October 2, 2015 analysis). Both downwind transects exhibit similar spatial plume features including the greatest ΔX_{CH_4} between about −92.7° and −92.2° longitude. These features are the direct result of the magnitude of CH_4 emissions at that longitude range given the relatively small variability in horizontal winds (see below). Downwind transect 1 CH_4 mole fractions at the transect edges are nearly identical to the transect edges upwind as expected because of nearly constant PBL height during this period (and associated small entrainment of cleaner air from the free troposphere) based on vertical profiles (Figure S8) and wind profiler data (Figure S2a). However, the mean background CH_4 mole fraction estimate based on the transect edges of the upwind and downwind 1 transects (purple horizontal bar indicating the 1σ uncertainty range in Figure S3) is greater than that of the full upwind transect because of nonuniform upwind CH_4 mole fractions. Unless the upwind nonuniformity is accounted for, downwind ΔX_{CH_4} and CH_4 emissions would be underestimated by 28% across the full downwind transect (see SI section 3). Note that it takes ∼2.3 h for the air mass upwind to travel to the downwind locations given the mean wind speed of 7.8 m/s (SI sections 5 and 6), which is consistent with a sampling time difference of 1.9 h between upwind and downwind transect 2. The sampling difference is smaller for downwind transect 2 (0.9 h), but Figure 2 shows that the shapes of downwind transects 1 and 2 are very similar, not indicating major temporal changes in upwind CH_4 entering the study area.

While there is currently no single established method for defining background CH_4 in the aircraft mass balance literature (see SI section 3), the majority of studies[2−5,7] do not fully account for nonuniform upwind CH_4 mole fractions. Instead, most studies would use a CH_4 background equivalent to the purple bar in Figure 2 (see details in SI section 3). In this study, we accounted for the observed nonuniform upwind CH_4 mole fractions by using a spatially varying CH_4 background (blue line in Figure 2) in the emission calculation, thereby including a spatially resolved estimate of CH_4 inflow into the study region compared to a constant background CH_4 value. The spatially varying CH_4 background was determined by longitudinally shifting the upwind CH_4 mole fractions based on daily mean horizontal wind direction and speed as well as distance between upwind and downwind transects. This technique for determining spatially resolved background CH_4 mole fractions assumes that the observed nonuniform upwind CH_4 was transported through the study area, thereby influencing the downwind CH_4 mole fractions. The particular conditions of this study, i.e., strong and consistent winds (7.8 m/s, 1.2° wind direction 1σ variability) and a relatively short upwind−downwind distance (65 km), facilitate the application of our method. We show its influence on the estimated CH_4 emissions quantitatively below.

In addition, note in Figure 2 that the downwind transect 2 western edge CH_4 mole fractions are ∼10 ppb lower than those of the downwind transect 2 eastern edge and both edges of downwind transect 1. One possible explanation is a longitudinal gradient in the PBL growth (more PBL growth in the west relative to the east) during downwind transects 1 and 2, and its associated entrainment of "cleaner" air from the free troposphere (see supporting data of water vapor and virtual potential temperature in Figure S10). Finally, we observed a sharp CH_4 spike (80 ppb, 1 km wide) during the upwind transect at −92.00° longitude/400 m AGL (estimated at 1.4 ± 0.6 t CH_4/h), and we detected a plume of the same magnitude (1.4 ± 0.4

DOI: 10.1021/acs.est.7b01810
Environ. Sci. Technol. 2017, 51, 7286−7294

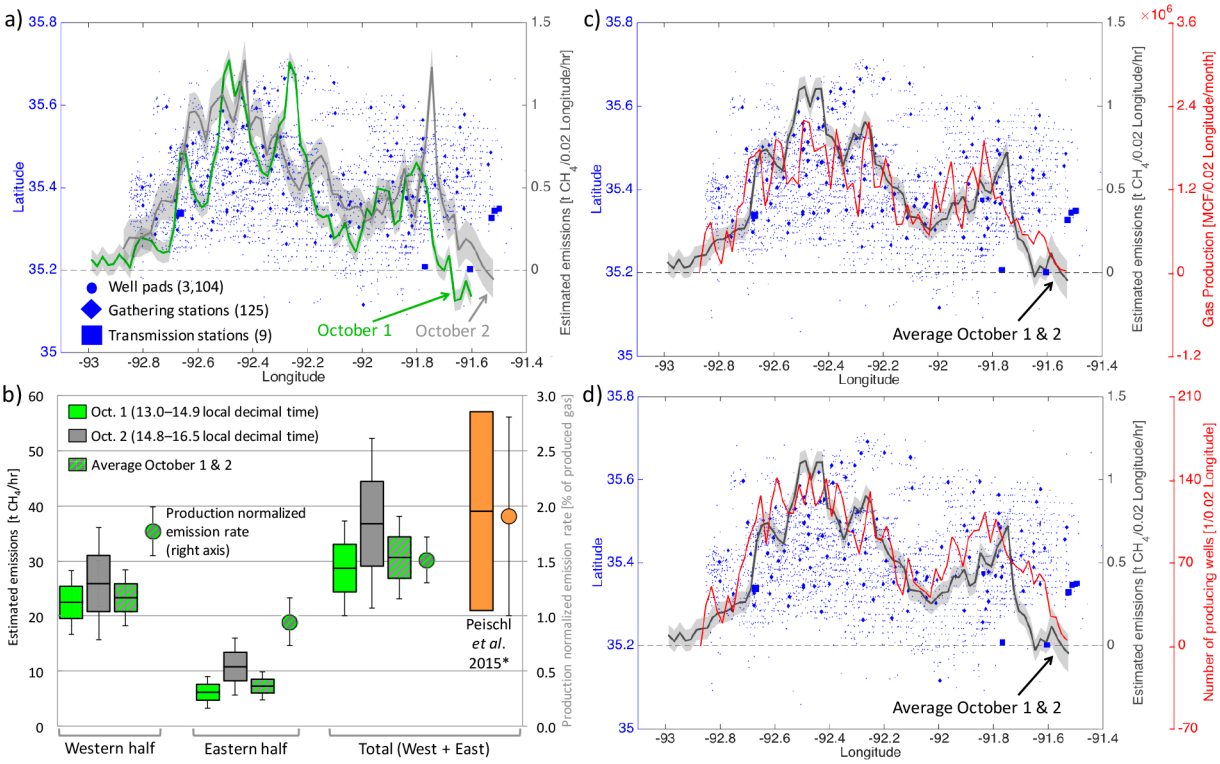

Figure 3. (a) Study area spatial (longitudinal) distribution of estimated total CH_4 emissions for each 0.02° longitude interval (shaded areas represent 1σ uncertainties) for October 1 and October 2 corrected for wind direction (see text and Figure S4a). (b) Comparison of October 1 and October 2 mean total CH_4 emissions (boxes, left y-axis; including western and eastern halves of study area divided at 92.1° longitude) and production normalized emission rates (PNER; circles, right y-axis) with a literature[6] estimate based on one aircraft mass balance flight in June 2013. PNER accounts for differences in gas production[23] between the flights (8% greater gas production in June 2013 than during our study). Emission boxes and whiskers indicate 1σ and 2σ uncertainties, respectively. PNER whiskers indicate 1σ uncertainties. (c) October 1 and 2 average CH_4 emissions (boxes are 1σ, whiskers are 2σ) in comparison with reported[23] study area NG production (red line) during our study period (see Figure S5 for comparison with producing gas well counts). (d) Same as panel c, but in comparison with the reported[23] number of producing NG wells (red line). *Note that the literature[6] estimate is only reported at 1σ, and the 2σ would encompass 3−75 t CH_4/h assuming a normal distribution. Local time indicates Central Daylight Time (UTC−5). Figure was produced using MATLAB.[43]

t CH_4/h; 40 ppb, 2 km wide) during downwind transect 3 at −92.01° longitude/980 m AGL (Figure S9), which supports our hypothesis that there is little lateral dispersion of upwind CH_4 and emissions as they travel southwards through the study area. The downwind location of this spike is consistent with the observed mean wind direction (from the north, 2° N ± 1°). This sharp CH_4 spike was most likely caused by an (unknown) episodic point source upwind of the study region because it was not detected on downwind transects 1 and 2 and the center transect directly following downwind transect 3 (and absence of this CH_4 spike on October 2; see SI section 2 for details).

Note that we did not use downwind transect 3 in the CH_4 emission quantification for two reasons: (i) A visible agricultural fire plume affected the study area east of −91.6° (15.8 CDT), which modified the CH_4 mole fractions otherwise included in the background determination (particularly for determining a potential longitudinal background gradient; Figure S9). (ii) The mean downwind transect 3 flight altitude (∼1020 m AGL) reached close to the PBL top (1350 ± 100 m AGL). Measured CH_4 mole fractions during some portions of the transect are thus diluted compared to downwind transects 1 and 2 (Figure S9). The data, figures, and descriptions for October 1 above are presented in a similar manner for the October 2 flight in SI section 2. The meteorological conditions including PBL height and average horizontal wind speed and direction were similar on both days (Table S1 and Table S2).

Spatially Resolved Study Area CH_4 Emission Estimates. Accounting for nonuniform upwind CH_4 and horizontal wind directions on each day, Figure 3a shows the estimated mean total CH_4 emissions including uncertainties as a function of longitude for both flights. The October 1 and 2, 2015 CH_4 emission estimates for a given 0.02° longitude interval refer to a swath of the same width, and each swath is parallel to the mean wind direction during that flight. Given the differences in the mean wind directions (2° N and 17° N on Oct 1 and Oct 2, respectively; Figure S4a), the longitudinal CH_4 emissions on both days refer to slightly different NG infrastructure footprints sampled (albeit with the same longitudinal center-point of each swath) as illustrated in more detail in Figure S4a.

Consistent with our companion paper's time-resolved bottom-up emission inventory,[17] the longitudinal CH_4 emission features show strong similarities between both days in the absence of substantial changes in the NG industry and non-NG sources. The maximum and minimum emissions occurred near −92.5° and −92.0° longitude (in addition to lateral edges), respectively, on both days, which is spatially similar to the observed downwind ΔX_{CH_4} pattern in Peischl et al.[6] in 2013. The estimated CH_4 emissions and the 1σ uncertainties near the edges of the study area mostly encompass zero as expected, and the few nonzero values (e.g., negative CH_4 emissions near −91.65° longitude on October 1) are explained by imperfect

DOI: 10.1021/acs.est.7b01810
Environ. Sci. Technol. 2017, 51, 7286−7294

Table 1. Study Area West−East Comparison of Natural Gas (NG) Infrastructure, CH_4 Emissions, Production Normalized Emission Rates (PNER), and Manual Liquid Unloading (MLU) Events (Active during the Downwind Transects; Ranges Indicate 1σ Uncertainty)

	gas production[a] [MCF/d]	active well count[a]	gathering station count[a]	transmission station count[a]	NG CH_4 emissions[b] [t CH_4/h]	PNER[c] [%]	active MLU events[d]	MLU CH_4 emissions[e] [t CH_4/h]	PNER excl. MLU CH_4 emissions[f] [%]
west	1.6×10^6	3520	84	1	21.5	1.7−2.0	15.8	7.0−10.6	0.8−1.4
east	0.8×10^6	1910	41	8	5.7	0.8−1.5	2.6	1.1−1.7	0.5−1.2
W−E ratio	2.0	1.8	2.0	0.1	3.8	**1.3−2.3**	6.2	6.2	**1.1−1.5**

[a]Data from ref 23. [b]Study area top-down CH_4 emission estimates (Figure 3, panel b, mean values) minus study area bottom-up non-NG sources CH_4 emission estimates (SI section 7, mean values). [c]October 1 and 2, 2015 range of mean values. [d]Industry study partner reported data (October 1 and 2, 2015 averages). [e]Based on d and range of bottom-up MLU emission rate estimates (see SI section 9). [f]PNER assuming no CH_4 emissions from MLU events (October 1 and 2, 2015 range of mean values).

agreement in background CH_4 levels between downwind transect edges and the upwind transect at individual locations. Note, however, the small magnitude of the negative values (e.g., a total of −0.4 t CH_4/h near −91.65° longitude on October 1).

The absence of substantial CH_4 emissions east of 91.7° longitude on October 1 (and October 2, see SI section 2) is confirmed by CH_4 measurements in Figure 2 (no substantial CH_4 plumes were detected there on both downwind transects irrespective of the choice of background CH_4 values). The difference in the mean CH_4 emissions in the same region between October 1 and October 2 was only 2 t CH_4/h, suggesting that it is indeed a low emitting region.

The October 1 and 2, 2015 average (and 1σ) longitudinal CH_4 emissions of all sources in the study area are shown in Figure 3c in comparison with reported[23] total NG production (summarized into 0.02° longitude bins) in the study area in September 2015 (latest data publicly available). There is general consistency between aircraft mass balance estimated longitudinal CH_4 emissions and longitudinal NG production including the local maxima near −92.5° and −91.8° longitude, the local minimum near −92.1° longitude, and the convergence to zero at the lateral edges. Figure 3d shows a similar longitudinal consistency between estimated CH_4 emissions and producing gas well count. A regression analysis (Figure S6) shows a correlation coefficient between longitudinally binned top-down CH_4 emissions estimates and reported[23] NG production of 0.75 (and 0.81 for producing well counts). The structural differences between emissions and NG production for individual longitudinal bins (explaining the imperfect correlation) may be due to multiple factors including (i) temporal approximation (production levels during the ∼5 h of flight on both days may differ from reported monthly average), (ii) emissions from local episodic CH_4 sources (see below), (iii) variability in facility-level CH_4 emissions, and (iv) non-NG related CH_4 emissions.

Figure 3b aggregates the longitudinal CH_4 emission estimates into the western and eastern halves of the study area (−92.1° longitude midpoint) and total study area. Accounting for nonuniform upwind CH_4 on both days, there is a 22% difference between mean hourly study area CH_4 emissions on October 1 (28.7 ± 4.3 t CH_4/h; 1σ) and October 2 (36.7 ± 7.7 t CH_4/h; 1σ). Yet, as illustrated in more detail in Figure S3, this difference would be much larger (47%) if assuming a uniform upwind CH_4 on each day (i.e., using only the downwind transect edges to determine background CH_4). Unless such large day-to-day total study area emission differences are expected based on operational changes in NG production, our treatment of the observed upwind CH_4 improves the accuracy of the study area aircraft emission estimation. Thus, our results show that adequately capturing CH_4 observations in the upwind PBL is critical to deriving an unbiased mass balance CH_4 emission estimate for the specific flight period.

The October 1 and 2, 2015 average hourly CH_4 emissions and uncertainties (see SI section 6 for uncertainty analysis) as well as the two-day uncertainty-weighted hourly average (30.6 ± 3.8 t CH_4/h; 1σ) fall in the 1σ uncertainty range (21−57 t CH_4/h) reported by Peischl et al.[6] based on a single flight day in 2013 (the unreported 2σ uncertainties would encompass 3−75 t CH_4/h assuming normal distributions). While the single day mean hourly estimate in Peischl et al.[6] is 8.4 t CH_4/h (or 27%) greater than our 2-day average, our difference between October 1 and 2, 2015 mean estimates is nearly the same (8.0 t CH_4/h). Inferring a multiyear temporal trend between both studies is not appropriate because (i) the single-day Peischl et al.[6] estimate may not be representative of average annual 2013 emissions given the large day-to-day emission differences shown here, (ii) there is substantial overlap in uncertainties between both studies, and (iii) gas production during the 2013 flight[6] was 8% greater than in 2015 (ref 23). The factor of 4 reduction in total CH_4 emission uncertainties relative to Peischl et al.[6] is due to (i) twice the number of downwind transects, (ii) more consistent winds during the flight (factor of 2 reduced uncertainty in horizontal wind speed perpendicular to flight track), and (iii) the use of wind profiler data in addition to aircraft vertical profiles (factor of 2 reduced uncertainty in PBL height estimate on October 1, 2015).

Study Area CH_4 Source Attribution and Production Normalized Emission Rates. We created a bottom-up estimate of CH_4 emissions from non-NG sources including enteric fermentation, a landfill, manure management, wastewater treatment, rice cultivation, a power plant, wetlands, and geologic seepage. Emissions from these sources contribute to total emissions in the study area and are encompassed by our estimated top-down emissions. As described in detail in SI section 7, our non-NG industry CH_4 emission estimate is based on (i) reported CH_4 emissions in the study area for some sources, (ii) literature emission factors for the remaining sources, and (iii) associated activity data (e.g., count of point sources and aerial extent for area sources). We estimated 3.4 ± 0.6 t CH_4/h (1σ) from non-NG industry sources, which is within uncertainties of Peischl et al.[6] (3.3 t CH_4/h; no uncertainties reported) albeit with substantially different individual non-NG source contributions.

We also estimated a production normalized emission rate (PNER), which is defined as the percentage of NG industry produced CH_4 released to the atmosphere (including vented

DOI: 10.1021/acs.est.7b01810
Environ. Sci. Technol. 2017, 51, 7286−7294

and fugitive emissions) in the study area. We subtracted the above spatially resolved non-NG CH_4 emissions from our study area mass balance CH_4 estimate, and we accounted for a mean NG CH_4 content of 91.6 ± 2.1 wt % (1σ; only 0.5 wt % difference between east and west based on industry study partner gas composition data). We assume that hourly NG production during the October 1 and 2, 2015 flights was representative of reported[23] monthly NG production (September 2015). As shown in Figure 3b, this results in a two-day (October 1 and 2, 2015) average PNER of 1.5 ± 0.2% (1σ) compared to 1.9 ± 0.9% (1σ) in a previous study.[6] As shown in Table 1 (and consistent with our regression analysis above), PNER in the western part (1.8 ± 0.2%; 1σ) is approximately double the PNER in the eastern part (0.9 ± 0.2%; 1σ). Table 1 also shows that the count of active gas wells, gathering stations, and transmission stations alone cannot explain the PNER west−east difference. Thus, NG operations in the western study area emit more CH_4 per gas throughput than in the eastern half during the flight windows on both days.

The Significance of Episodic Emission Sources. Further analysis shows that emissions from manually triggered liquid unloadings (MLU), which help resume gas flow at wells where water or other liquids have accumulated in the well bore, could help explain the west−east PNER difference. We estimated CH_4 emissions from MLU events using a bottom-up approach based on (i) the start and end times of each of the 107 total MLU events on October 1 and 2, 2015 reported by local NG industry operators (which represent 99% of all active wells in the study area) and (ii) measured MLU CH_4 emission rates from eight wells of the same type and geographic region by Allen et al.[35]

As described in detail in SI section 9, and summarized in Table 1, MLU alone accounts for 8−12 t CH_4/h in the study area (30−46% of our top-down two-day mean estimate excluding non-NG sources) during the midday flight windows on October 1 and 2, 2015. The west−east ratio of the active MLU events (concurrent with the aircraft downwind transects) is 6.2, compared to a west−east ratio of total NG CH_4 emissions of only 3.8. Our bottom-up estimates of MLU associated CH_4 emissions thus explain 42−90% of the difference in PNER between west and east (two-day weighted average). Our bottom-up MLU CH_4 emission estimates may not be considered definitive without further research (e.g., regarding the representativeness of the eight Allen et al.[35] measurements for the reported 107 MLU events, and potentially additional MLU events by nonstudy partners). However, our estimated order of magnitude of MLU CH_4 emissions suggests that MLU events likely contribute substantially to the west−east PNER difference.

■ DISCUSSION

The aircraft mass balance technique leverages high precision, high accuracy measurements of the PBL CH_4 mole fractions upwind and downwind of the study area, as well as PBL height and horizontal wind speed and direction in the PBL. Variability and uncertainty in these observations used in the estimation model (see Materials and Methods, eq 1) are combined explicitly to derive uncertainties for the estimated emissions independently of bottom-up inventories (SI section 6). We were able to reduce CH_4 emission uncertainties substantially (factor of 4) relative to a previous study[6] over the same region by doubling the number of sampled transects, employing a wind profiler, and because of favorable meteorological conditions (clear sky and low variability in PBL horizontal winds throughout the study area on both flight days). We suggest employing a wind profiler in future measurement campaigns as has been done in some previous campaigns[4,5,9] to reduce emission uncertainties.

We have refined the implementation of the aircraft mass balance quantification in three ways. The first refinement is an in-depth exploration of the sensitivity of downwind ΔX_{CH_4} and total CH_4 emissions to the definition of background CH_4 entering the study area. We find that fully accounting for the nonuniform upwind CH_4 in calculating downwind ΔX_{CH_4} reduces the difference in estimated CH_4 emissions between two consecutive days (both total and spatially resolved emissions) by a factor of more than 2. This bias correction is consistent with study partner reported activity data. Second, we accounted for wind speed gradients in the vertical (using wind profiler data) and the horizontal (using aircraft data). This prevented a low bias of 10% of total CH_4 emissions on October 1, 2015 (negligible impact on October 2, 2015). Third, the detailed accounting of background CH_4 and wind speed gradients allowed us to quantify for the first time spatially resolved CH_4 emissions of a NG producing basin. While beyond the scope of this study, statistical inverse models could provide additional emission estimates for flights with less optimal meteorological conditions, but they introduce additional uncertainties, which are sometimes difficult to quantify and interpret.[36]

Implications for Interpreting Aircraft Measurements. The significant agreement in the longitudinal patterns of aircraft estimated CH_4 emissions on two consecutive days with reported NG production (R^2 = 0.75) and well pad count (R^2 = 0.81) provides supportive evidence that the aircraft mass balance is a valid, quantitative, and independent approach to estimate aggregated methane emissions on the mesoscale including NG producing basins. Previous studies[10,37] found that NG production is a weak predictor of CH_4 emissions for individual well pads based on helicopter- and ground-based measurements. This is based on the observation that CH_4 emissions of any individual well pad at a given point in time do not correlate well with NG production. However, we show that there can be a strong correlation between CH_4 emissions and publicly available data[23] on NG production (and well count) at the sub-basin level in a dry shale gas basin. The spatial estimates described here will allow a detailed comparison and evaluation of a temporally and spatially consistent bottom-up emission inventory[17] based on facility- and component-level measurements[38,39] combined with a complete inventory of NG infrastructure and large emission events in the study area.

An improved mechanistic understanding of emissions on the facility and basin scale is critical to improving the accuracy of regional and national scale inventories and top-down inverse model studies. Our study based on state of the science measurements, analysis, and access to industry operational data is unique and sheds new light on the interpretation of previous basin scale aircraft studies. The interpretation of previous short-term, midday aircraft-based CH_4 measurements has focused on comparison with annualized inventories. Some[18,40−42] have employed statistical models to explain differences between top-down and bottom-up estimates with the existence of super-emitters or unknown sources of emissions, i.e., fat tail emission distributions. We offer a different explanation by showing that manually triggered, episodic releases of NG can represent a

DOI: 10.1021/acs.est.7b01810
Environ. Sci. Technol. 2017, 51, 7286−7294

large fraction (~1/3 in this case) of total midday CH_4 emissions. This explanation is based on average emission rates of the specific episodic releases (MLU) rather than statistical fat tails. Thus, a valid comparison of aircraft estimates with annualized inventories needs to establish the representativeness of midday activity data for annualized emissions as done in our companion paper.[17] Episodic releases, rather than atmospheric variability, may also explain substantial day-to-day variability.

■ ASSOCIATED CONTENT

Supporting Information

The Supporting Information is available free of charge on the ACS Publications website at DOI: 10.1021/acs.est.7b01810.

Contains description of additional measurements, more detailed data/uncertainty analysis of all measurements, calculation of non-natural gas CH_4 emissions, and calculation/analysis of production normalized emission rates (PNER) (PDF)

■ AUTHOR INFORMATION

Corresponding Author

*Phone: (303) 497-5073. E-mail: stefan.schwietzke@noaa.gov.

ORCID

Stefan Schwietzke: 0000-0002-1836-8968

Stephen Conley: 0000-0001-6753-8962

Daniel Zimmerle: 0000-0003-2832-048X

Notes

The authors declare the following competing financial interest(s): The authors declare no personal competing financial interest. Research funding provided via cost share from institutions associated with the oil and gas industry is as described in the Acknowledgments.

■ ACKNOWLEDGMENTS

Funding for this work was provided by RPSEA/NETL contract no 12122-95/DE-AC26-07NT42677 to the Colorado School of Mines. Cost share for this project was provided by Colorado Energy Research Collaboratory, the National Oceanic and Atmospheric Administration, Southwestern Energy, XTO Energy, a subsidiary of ExxonMobil, Chevron, Statoil, and the American Gas Association, many of whom also provided operational data and/or site access. Additional data and/or site access was also provided by CenterPoint, Enable Midstream Partners, Kinder Morgan, and BHP Billiton. We thank our Science Advisory Panel members K. Davis, S. Hanna, D. Allen, D. Cooley, and A. Brandt as well as A. Karion, G. Etiope, R. Klusman, and W. Angevine for valuable comments. Archived wind profiler data products are available at http://www.esrl.noaa.gov/psd/data/obs/cgi-bin/GetArchive.pl?source=UneditedNonActive. We thank the Little Rock, AR National Weather Service forecast office for providing daily weather briefings during the measurement campaign. We thank the South Side Bee Branch High School for kindly providing a siting location for the NOAA wind profiler.

■ REFERENCES

(1) EPA Releases First-Ever Standards to Cut Methane Emissions from the Oil and Gas Sector. https://www.epa.gov/newsreleases/epa-releases-first-ever-standards-cut-methane-emissions-oil-and-gas-sector.

(2) Smith, M. L.; Kort, E. A.; Karion, A.; Sweeney, C.; Herndon, S. C.; Yacovitch, T. I. Airborne Ethane Observations in the Barnett Shale: Quantification of Ethane Flux and Attribution of Methane Emissions. *Environ. Sci. Technol.* **2015**, *49* (13), 8158−8166.

(3) Peischl, J.; Karion, A.; Sweeney, C.; Kort, E. A.; Smith, M. L.; Brandt, A. R.; Yeskoo, T.; Aikin, K. C.; Conley, S. A.; Gvakharia, A.; et al. Quantifying atmospheric methane emissions from oil and natural gas production in the Bakken shale region of North Dakota. *J. Geophys. Res. Atmos* **2016**, *121* (10), 6101−6111.

(4) Karion, A.; Sweeney, C.; Kort, E. A.; Shepson, P. B.; Brewer, A.; Cambaliza, M.; Conley, S. A.; Davis, K.; Deng, A.; Hardesty, M.; et al. Aircraft-Based Estimate of Total Methane Emissions from the Barnett Shale Region. *Environ. Sci. Technol.* **2015**, *49* (13), 8124−8131.

(5) Karion, A.; Sweeney, C.; Pétron, G.; Frost, G.; Michael Hardesty, R.; Kofler, J.; Miller, B. R.; Newberger, T.; Wolter, S.; Banta, R.; et al. Methane emissions estimate from airborne measurements over a western United States natural gas field. *Geophys. Res. Lett.* **2013**, *40* (16), 4393−4397.

(6) Peischl, J.; Ryerson, T. B.; Aikin, K. C.; De Gouw, J. A.; Gilman, J. B.; Holloway, J. S.; Lerner, B. M.; Nadkarni, R.; Neuman, J. A.; Nowak, J. B.; et al. Quantifying atmospheric methane emissions from the Haynesville, Fayetteville, and northeastern Marcellus shale gas production regions. *J. Geophys. Res. D Atmos* **2015**, *120* (5), 2119−2139.

(7) Kort, E. A.; Smith, M. L.; Murray, L. T.; Gvakharia, A.; Brandt, A. R.; Peischl, J.; Ryerson, T. B.; Sweeney, C.; Travis, K. Fugitive emissions from the Bakken shale illustrate role of shale production in global ethane shift. *Geophys. Res. Lett.* **2016**, *43* (9), 4617−4623.

(8) Schwarz, J. P.; Holloway, J. S.; Katich, J. M.; McKeen, S.; Kort, E. A.; Smith, M. L.; Ryerson, T. B.; Sweeney, C.; Peischl, J. Black Carbon Emissions from the Bakken Oil and Gas Development Region. *Environ. Sci. Technol. Lett.* **2015**, *2* (10), 281−285.

(9) Pétron, G.; Karion, A.; Sweeney, C.; Miller, B. R.; Montzka, S. A.; Frost, G. J.; Trainer, M.; Tans, P.; Andrews, A.; Kofler, J.; et al. A new look at methane and nonmethane hydrocarbon emissions from oil and natural gas operations in the Colorado Denver-Julesburg Basin. *J. Geophys. Res. Atmos* **2014**, *119* (11), 6836−6852.

(10) Brantley, H. L.; Thoma, E. D.; Squier, W. C.; Guven, B. B.; Lyon, D. Assessment of methane emissions from oil and gas production pads using mobile measurements. *Environ. Sci. Technol.* **2014**, *48* (24), 14508−14515.

(11) Mitchell, A. L.; Tkacik, D. S.; Roscioli, J. R.; Herndon, S. C.; Yacovitch, T. I.; Martinez, D. M.; Vaughn, T. L.; Williams, L. L.; Sullivan, M. R.; Floerchinger, C.; et al. Measurements of Methane Emissions from Natural Gas Gathering Facilities and Processing Plants: Measurement Results. *Environ. Sci. Technol.* **2015**, *49* (5), 3219−3227.

(12) Allen, D. T.; Torres, V. M.; Thomas, J.; Sullivan, D. W.; Harrison, M.; Hendler, A.; Herndon, S. C.; Kolb, C. E.; Fraser, M. P.; Hill, a D.; et al. Measurements of methane emissions at natural gas production sites in the United States. *Proc. Natl. Acad. Sci. U. S. A.* **2013**, *110* (44), 17768−17773.

(13) Pétron, G.; Frost, G.; Miller, B. R.; Hirsch, A. I.; Montzka, S. A.; Karion, A.; Trainer, M.; Sweeney, C.; Andrews, A. E.; Miller, L.; et al. Hydrocarbon emissions characterization in the Colorado Front Range: A pilot study. *J. Geophys. Res. Atmos* **2012**, *117* (D4), D04304.

(14) Harrison, M. R.; Shires, T. M.; Wessels, J. K.; Cowgill, R. M. *Methane Emission from the Natural Gas Industry*; U.S. EPA: Research Triangle Park, NC, 1997.

(15) *Inventory of U.S. Greenhouse Gas Emissions and Sinks: 1990 − 2014*; U.S. Environmental Protection Agency: Washington, DC, 2016.

(16) Brandt, A. R.; Heath, G. A.; Kort, E. A.; O'Sullivan, F.; Pétron, G.; Jordaan, S. M.; Tans, P.; Wilcox, J.; Gopstein, A. M.; Arent, D.; et al. Methane Leaks from North American Natural Gas Systems. *Science* **2014**, *343* (6172), 733−735.

(17) Vaughn, T. L.; Bell, C.; Pickering, C.; Heath, G.; Murphy, S. M.; Petron, G.; Robertson, A. M.; Pickering, C.; Roscioli, J. R.; Yacovitch, T. I.; et al. Reconciliation of regional methane emissions: Systematic analysis of facility-level methane emissions measured with multiple methods and comparison to simultaneous overflight mass balance measurements. Manuscript in preparation, **2017**.

DOI: 10.1021/acs.est.7b01810
Environ. Sci. Technol. 2017, 51, 7286−7294

(18) Zavala-Araiza, D.; Lyon, D. R.; Alvarez, R. A.; Davis, K. J.; Harriss, R.; Herndon, S. C.; Karion, A.; Kort, E. A.; Lamb, B. K.; Lan, X.; et al. Reconciling divergent estimates of oil and gas methane emissions. *Proc. Natl. Acad. Sci. U. S. A.* **2015**, *112* (51), 15597−15602.
(19) Turnbull, J. C.; Karion, A.; Fischer, M. L.; Faloona, I.; Guilderson, T.; Lehman, S. J.; Miller, B. R.; Miller, J. B.; Montzka, S.; Sherwood, T.; et al. Assessment of fossil fuel carbon dioxide and other anthropogenic trace gas emissions from airborne measurements over Sacramento, California in spring 2009. *Atmos. Chem. Phys.* **2011**, *11* (2), 705−721.
(20) Shankar Rao, K. Source estimation methods for atmospheric dispersion. *Atmos. Environ.* **2007**, *41* (33), 6964−6973.
(21) U.S. Shale gas production statistics. https://www.eia.gov/dnav/ng/ng_prod_shalegas_s1_a.htm.
(22) Zavala-Araiza, D.; Allen, D. T.; Harrison, M.; George, F. C.; Jersey, G. R. Allocating methane emissions to natural gas and oil production from shale formations. *ACS Sustainable Chem. Eng.* **2015**, *3* (3), 492−498.
(23) Fayetteville Shale Gas Sales Information. http://aogc2.state.ar.us/Fayshale/Default.aspx.
(24) Mielke-Maday, I.; Schwietzke, S.; Thorley, E.; Yacovitch, T.; Conley, S.; Kofler, J.; Handley, P.; Miller, B.; Hall, B.; Dlugokencky, E.; et al. Methane source attribution in a US dry gas basin using spatial patterns of ground and airborne ethane and methane measurements. Manuscript in preparation, **2017**.
(25) Conley, S.; Faloona, I.; Mehrotra, S.; Suard, M.; Lenschow, D. H.; Sweeney, C.; Herndon, S.; Schwietzke, S.; Pétron, G.; Pifer, J.; et al. Application of Gauss's Theorem to quantify localized surface emissions from airborne measurements of wind and trace gases. *Atmos. Meas. Technol. Discuss.* **2017**, 1−29.
(26) Scientific Aviation. http://scientificaviation.com.
(27) Conley, S. A.; Faloona, I. C.; Lenschow, D. H.; Karion, A.; Sweeney, C. A Low-Cost System for Measuring Horizontal Winds from Single-Engine Aircraft. *J. Atmos. Ocean. Technol.* **2014**, *31* (6), 1312−1320.
(28) Rella, C. W.; Chen, H.; Andrews, A. E.; Filges, A.; Gerbig, C.; Hatakka, J.; Karion, A.; Miles, N. L.; Richardson, S. J.; Steinbacher, M.; et al. High accuracy measurements of dry mole fractions of carbon dioxide and methane in humid air. *Atmos. Meas. Tech.* **2013**, *6* (3), 837−860.
(29) Dlugokencky, E. J.; Myers, R. C.; Lang, P. M.; Masarie, K. A.; Crotwell, A. M.; Thoning, K. W.; Hall, B. D.; Elkins, J. W.; Steele, L. P. Conversion of NOAA atmospheric dry air CH4 mol fractions to a gravimetrically prepared standard scale. *J. Geophys. Res.* **2005**, *110* (D18), D18306.
(30) *Methane WMO Scale Update: WMO X2004A*; NOAA Global Monitoring Division: Boulder, CO.
(31) Yacovitch, T. I.; Herndon, S. C.; Roscioli, J. R.; Floerchinger, C.; McGovern, R. M.; Agnese, M.; Pétron, G.; Kofler, J.; Sweeney, C.; Karion, A.; et al. Demonstration of an Ethane Spectrometer for Methane Source Identification. *Environ. Sci. Technol.* **2014**, *48* (14), 8028−8034.
(32) Carter, D. A.; Gage, K. S.; Ecklund, W. L.; Angevine, W. M.; Johnston, P. E.; Riddle, A. C.; Wilson, J.; Williams, C. R. Developments in UHF lower tropospheric wind profiling at NOAA's Aeronomy Laboratory. *Radio Sci.* **1995**, *30* (4), 977−1001.
(33) Bianco, L.; Wilczak, J. M.; White, A. B. Convective boundary layer depth estimation from wind profilers: Statistical comparison between an automated algorithm and expert estimations. *Journal of Atmospheric and Oceanic Technology* **2008**, *25*, 1397−1413.
(34) White, W. H.; Anderson, J. a; Blumenthal, D. L.; Husar, R. B.; Gillani, N. V.; Husar, J. D.; Wilson, W. E. Formation and transport of secondary air pollutants: ozone and aerosols in the St. Louis urban plume. *Science* **1976**, *194* (4261), 187−189.
(35) Allen, D. T.; Sullivan, D. W.; Zavala-Araiza, D.; Pacsi, A. P.; Harrison, M.; Keen, K.; Fraser, M. P.; Daniel Hill, A.; Lamb, B. K.; Sawyer, R. F.; Seinfeld, J. H.; et al. Methane Emissions from Process Equipment at Natural Gas Production Sites in the United States: Liquid Unloadings. *Environ. Sci. Technol.* **2015**, *49* (1), 641−648.
(36) Bruhwiler, L.; Dlugokencky, E.; Masarie, K.; Ishizawa, M.; Andrews, A.; Miller, J.; Sweeney, C.; Tans, P.; Worthy, D. CarbonTracker-CH4: An assimilation system for estimating emissions of atmospheric methane. *Atmos. Chem. Phys.* **2014**, *14* (16), 8269−8293.
(37) Lyon, D. R.; Alvarez, R. A.; Zavala-Araiza, D.; Brandt, A. R.; Jackson, R. B.; Hamburg, S. P. Aerial Surveys of Elevated Hydrocarbon Emissions from Oil and Gas Production Sites. *Environ. Sci. Technol.* **2016**, *50* (9), 4877−4886.
(38) Bell, C. S.; Vaughn, T. L.; Daube, C.; Edie, R.; Field, R. A.; Heath, G. A.; Herndon, S. C.; Knighton, W. B.; Murphy, S. M.; Pétron, G.; et al. Comparison of Methane Emission Estimates from Multiple Measurement Techniques at Natural Gas Production Pads. In review, **2017**.
(39) Vaughn, T. L.; Bell, C. S.; Yacovitch, T. I.; Roscioli, J. R.; Herndon, S. C.; Conley, S.; Schwietzke, S.; Heath, G. A.; Pétron, G.; Zimmerle, D. Comparing Facility-Level Methane Emission Rate Estimates at Natural Gas Gathering and Boosting Stations. In review, **2017**.
(40) Zavala-Araiza, D.; Alvarez, R. A.; Lyon, D. R.; Allen, D. T.; Marchese, A. J.; Zimmerle, D. J.; Hamburg, S. P. Super-emitters in natural gas infrastructure are caused by abnormal process conditions. *Nat. Commun.* **2017**, *8*, 14012.
(41) Brandt, A. R.; Heath, G. A.; Cooley, D. Methane Leaks from Natural Gas Systems Follow Extreme Distributions. *Environ. Sci. Technol.* **2016**, *50* (22), 12512−12520.
(42) Littlefield, J. A.; Marriott, J.; Schivley, G. A.; Skone, T. J. Synthesis of recent ground-level methane emission measurements from the U.S. natural gas supply chain. *J. Cleaner Prod.* **2017**, *148*, 118−126.
(43) Matlab Release 2014b; The Mathworks, Inc.: Natick, MA.

DOI: 10.1021/acs.est.7b01810
Environ. Sci. Technol. 2017, 51, 7286−7294